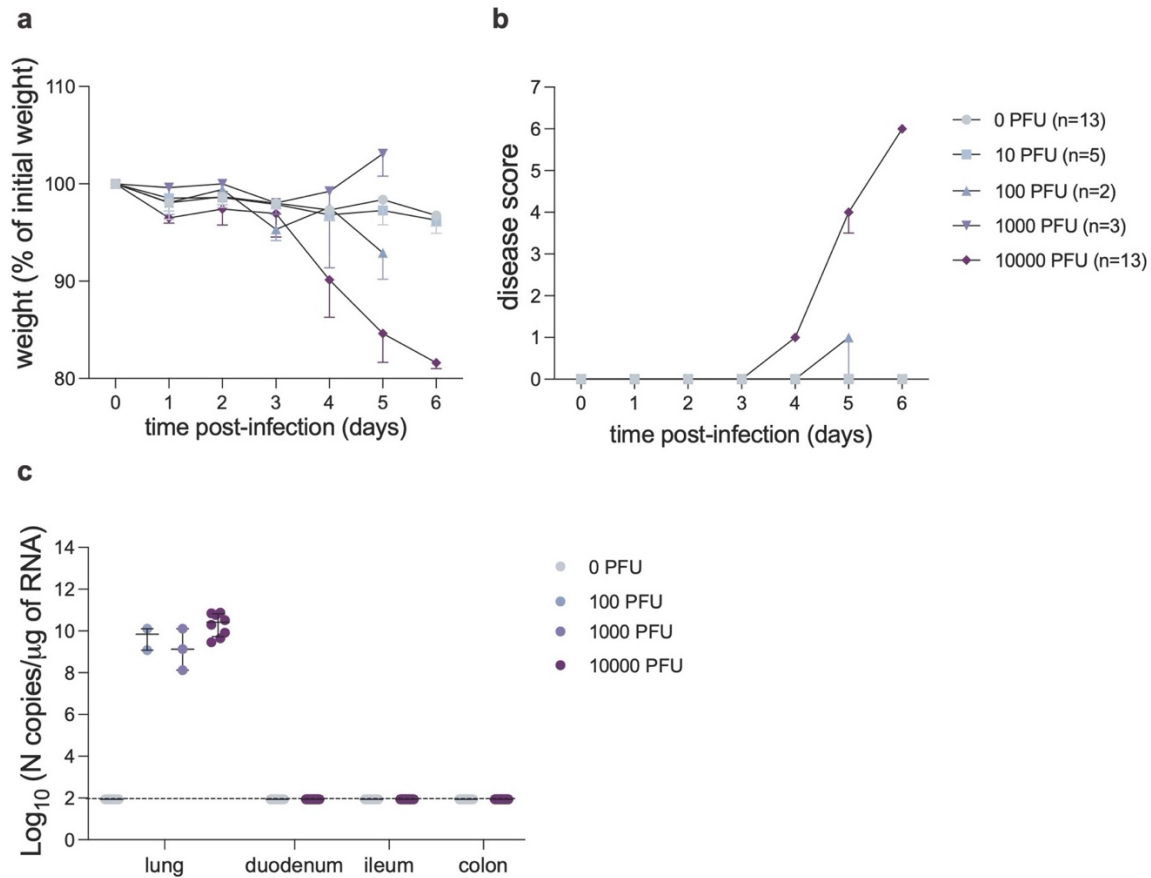


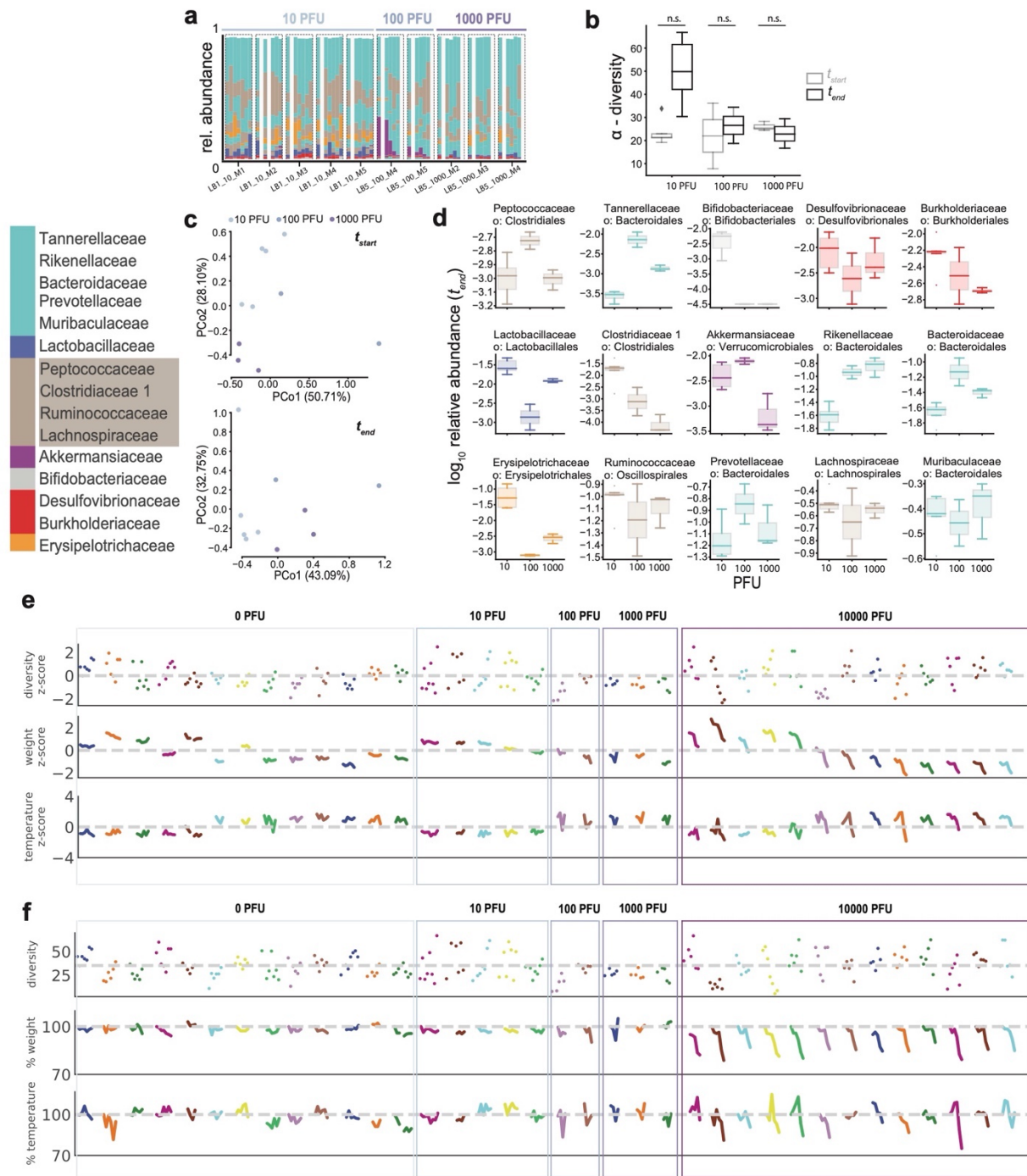
Supporting Information



824
825

826 **Extended Data Fig. S1 SARS-CoV-2 infection in K18-hACE2 mice.**

827 **a-b.** Following inoculation with 0, 10, 100, 1000 or 10000 PFU of SARS-CoV-2 or mock
828 infection, mice were monitored daily for weight loss (a) and signs of disease quantified by a
829 composite score based on ruffled fur, hunched back, heavy breathing and absence of mobility
830 (b). Median and interquartile range determined for each group at each time point are depicted.
831 Results are pooled from 1-3 independent experiments. For each group, the total number of mice
832 is indicated. c. Viral burden in lung or intestinal tissue of K18-hACE2 mice was analyzed at 5-6
833 days after infection with 100, 1000, 10000 PFU of SARS-CoV-2 or mock infection by qRT-
834 PCR. Dots represent the copy number of N RNA per μg of RNA calculated for each mouse.
835 Results were pooled from 1 (100 and 1000 PFU doses) or 2 (mock and 10000 PFU) independent
836 experiments with n=2-5 mice per group for each experiment. The median and interquartile range
837 are depicted for each experimental group. The dotted line depicts the limit of detection.



838

839

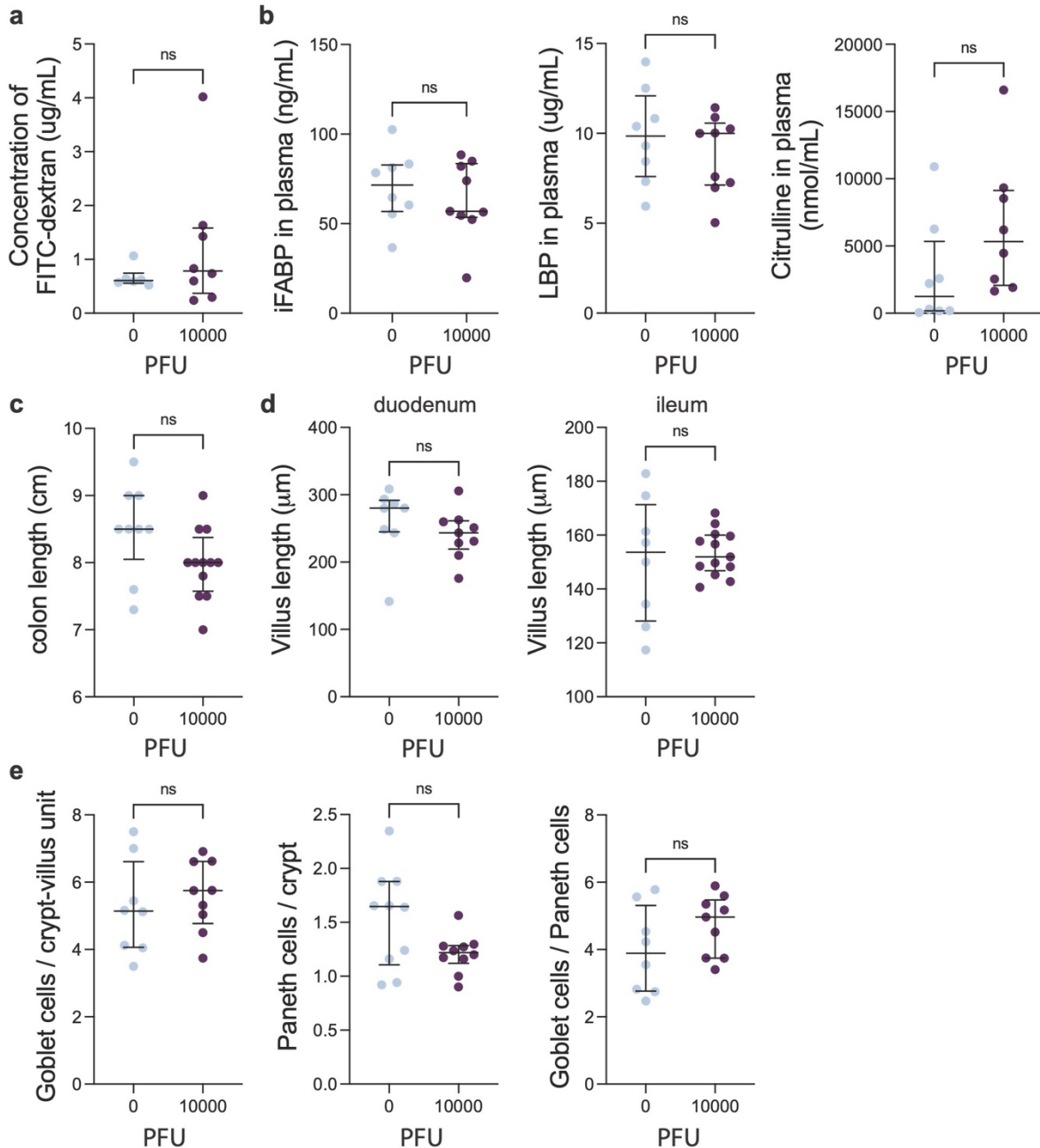
840

841 **Extended Data Fig. S2 Inconsistent microbiomes dynamics in mice with lower infection**

842 **doses. a** Bars represent bacterial family compositions in stool samples collected from mice over

843 time, mouse time courses grouped as indicated by boxes. **b** bacterial alpha diversity in first (t_{start})

844 and last (t_{end}) samples collected. **c** principal coordinate plots of bacterial compositions in first and
845 last samples colored by infection dose (in PFU). **d** bacterial family abundances by infection dose
846 at the final sample collected. **E** diversity, weight and temperature z-scores (calculated from all
847 data points) over time per mouse as shown in a and Fig. 1. **F** untransformed diversity, weights
848 and temperatures relative to the beginning of the experiment.
849
850



851

852

853 **Extended Data Fig. S3 Some intestinal parameters are not modified during SARS-CoV-2**

854 **infection.** K18-hACE2 mice were analyzed on day 5-6 post intranasal inoculation with 10000 PFU

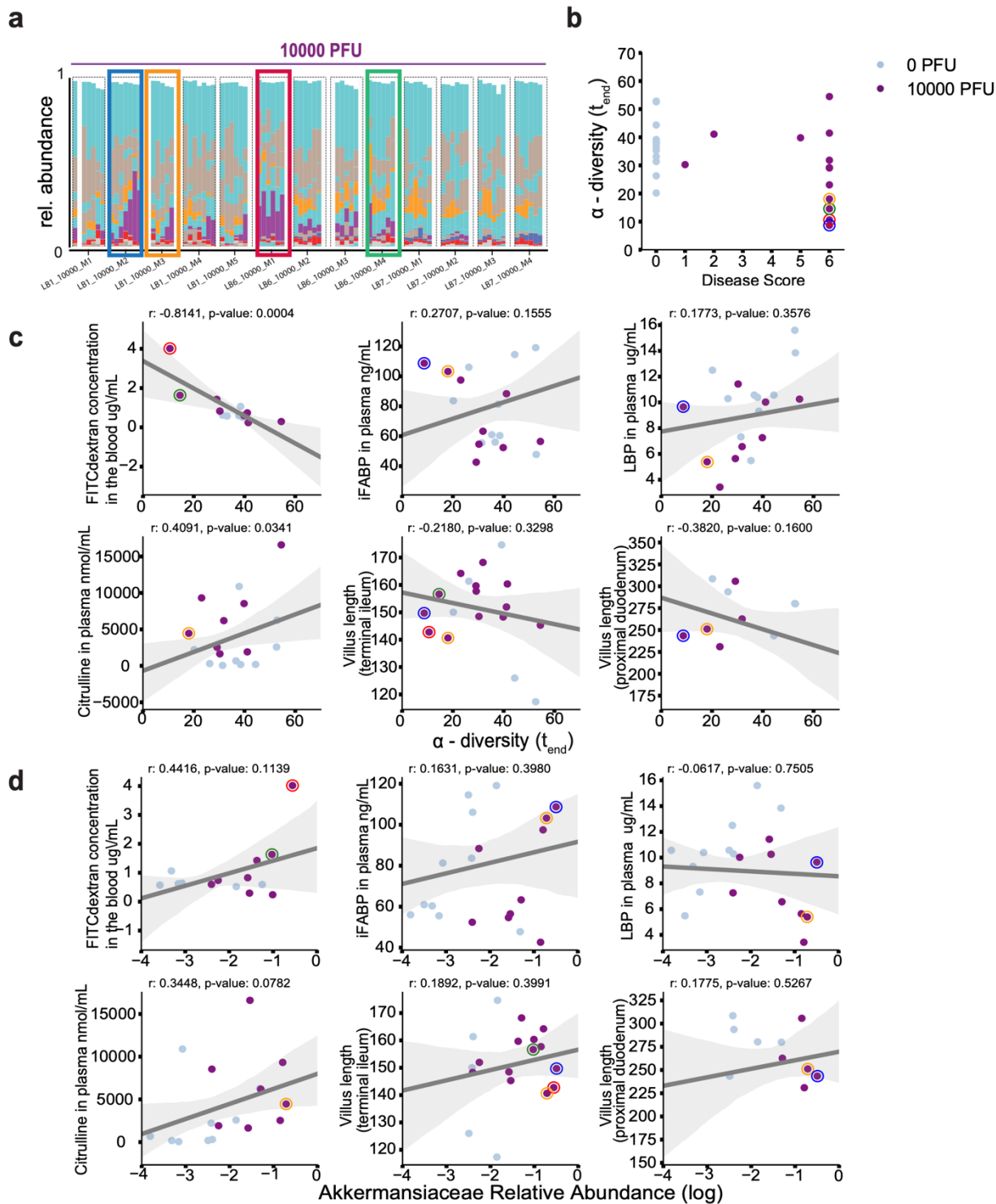
855 SARS-CoV-2 or mock treatment. **a.** Quantification of fluorescence intensity in the blood following

856 oral administration of FITC-dextran. **B.** Intestinal fatty acid-binding protein (iFABP), LPS-binding

857 protein (LBP), and citrulline concentration in plasma. **C.** Quantification of colon length. **d.**

858 Quantification of villus length in the duodenum (left) and ileum (right) based on H&E staining. **E.**

859 Quantification of goblet cell number (left) and Paneth cell number (middle) per crypt-villus unit
860 in the proximal duodenum based on H&E staining and calculation of goblet cell per Paneth cell
861 ratio based on these quantifications (right). Individual mice, represented by the circles as well as
862 the median and interquartile ranges are depicted. In d, e, each circle shows the mean for each
863 mouse of the cell number counted per crypt-villus unit on 50 units. Results were pooled from 2
864 (for a) or 3 independent experiments with n=3-5 mice per group for each experiment. Significant
865 differences were determined using the Mann-Whitney U test (ns=non-significant, $p > 0.05$; **,
866 $p < 0.01$; ***, $p < 0.001$; ****, $p < 0.0001$).

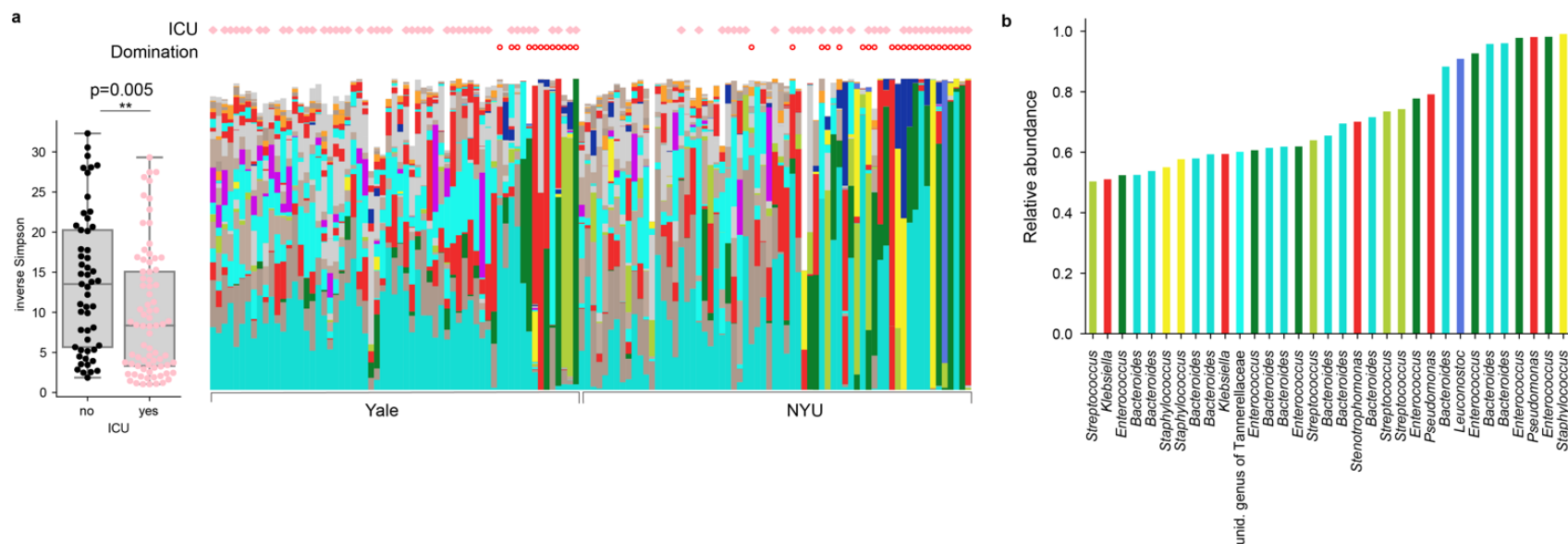


867
868

869 **Extended Data Fig. S4 Strongest gut dysbiosis is correlated with markers of defects in the**
870 **intestinal barrier and epithelium.** A Reproduction of Fig. 1 showing bacterial compositions in
871 mice infected with 10^4 PFUs, highlighting four mice time courses of mice with lowest diversity

872 and highest disease scores at the end of the experiment (**b**). **c-d** Correlations between alpha
873 diversity (**c**) (inverse Simpson) and \log_{10} relative *Akkermansia* abundances (**d**) at the end of the
874 experiment with epithelium phenotypes and gut barrier integrity markers measured in the blood
875 of mice (data from mice highlighted in **a** with circles in corresponding colors, lines: linear
876 regression, shaded region: 95%CI).
877
878

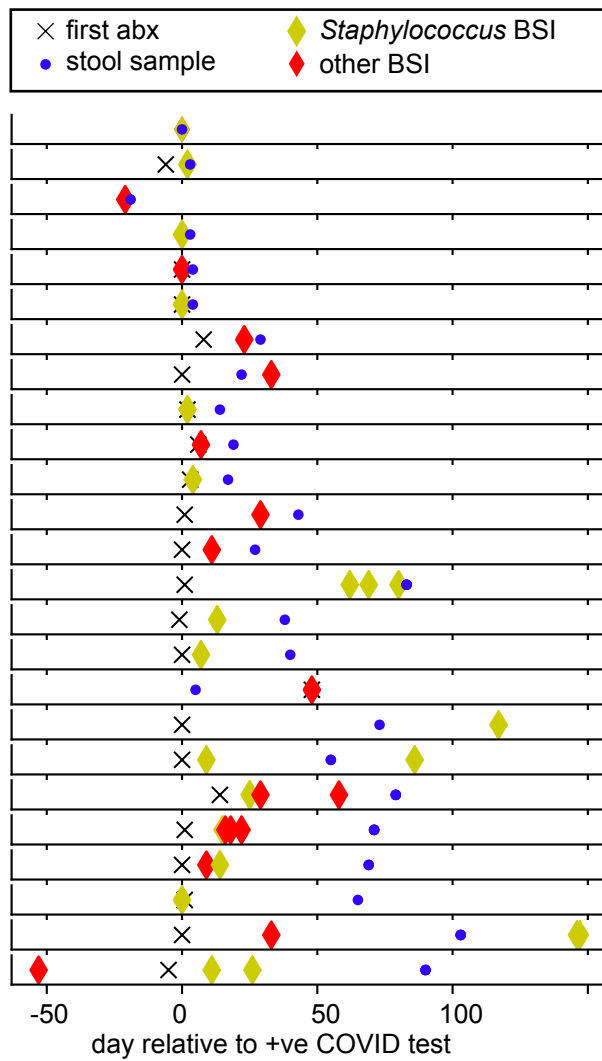
879



880

881 **Extended Data Fig. S5 a** Samples from patients requiring ICU transfer have lower diversity on average ($p=0.005$, Wilcoxon rank-
882 sum); bars as in Fig. 1 with ICU status of patients and domination state of samples indicated. **b** Genus abundances in samples with a
883 single genus $>50\%$ relative abundance.

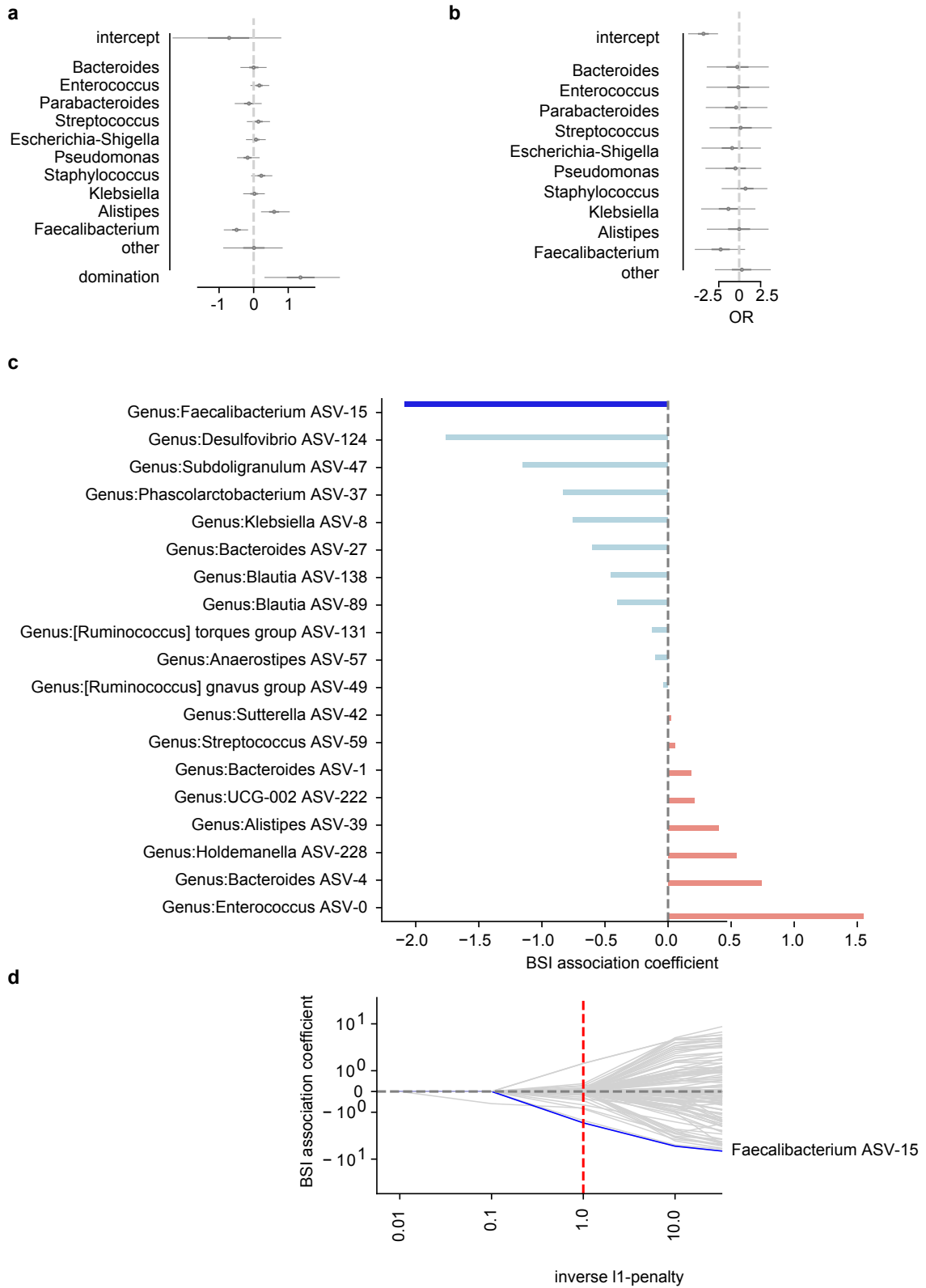
884



885

886 **Extended Data Fig. S6** Patients with a positive clinical blood culture result (BSI) received
887 antibiotics, prior or on the day of blood culture results (cross symbol: first recorded antibiotic
888 administration, blue: sequenced stool sample, diamond: positive blood culture result (BSI)).

889

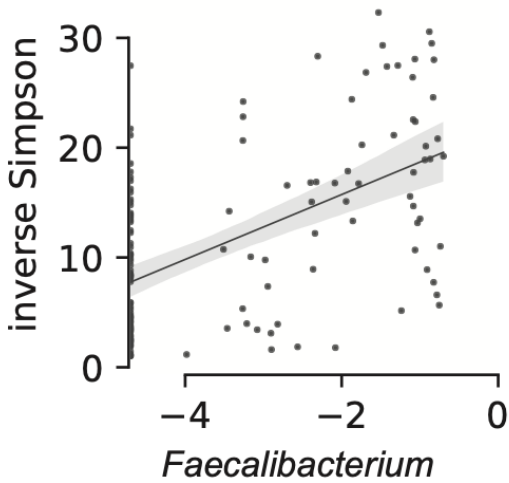


890

891 **Extended Data Fig. S7 a** Posterior coefficient estimates from a Bayesian logistic regression

892 regressing \log_{10} relative abundances of the top 10 most abundant bacterial genera on BSI status

893 using only BSI cases with associated stool samples taken prior or on the day of a confirmed
894 positive blood culture. **b** Posterior coefficient estimates from a Bayesian logistic regression
895 regressing \log_{10} relative abundances of the top 10 most abundant bacterial genera on BSI status
896 with domination status of the microbiome as an additional predictor (domination: >50% of the
897 composition by one taxon). **c** ASVs associated with samples from patients with BSI. Coefficients
898 from a cross-validated, L1-penalized logistic regression correlating the binary outcome (BSI)
899 with \log_{10} -transformed relative ASV abundances. **d** Cross-validation paths; for all regularization
900 strengths (L1-penalty) used, a *Faecalibacterium* ASV was most negatively associated with BSI-
901 positive samples.



902

903

904 **Extended Data Fig. S8 *Faecalibacterium* relative abundance is positively correlated with**

905 **bacterial alpha diversity.** Log10 transformed relative abundances of the genus

906 *Faecalibacterium* in stool samples from patients are correlated with the inverse Simpson

907 diversity index; line from linear regression, shaded region: 95%CI.

911 family compositions in stool samples; multiple samples belonging to the same patient grouped
912 by a white box. Two samples with matching whole genome sequenced (WGS) blood isolates
913 indicated. **b** Rank analysis of abundance patterns in stool samples from different BSI categories;
914 a filled circle indicates the calculated rank of the focal BSI category (row) in terms of the
915 corresponding taxon stool abundance relative to samples from other BSI categories (Lact:
916 Lactobacillales, Enbct: Enterobacterales; Pseu: Pseudomonadales, Bact: Bacteroidales, Staph:
917 Staphylococcales. Only 5 out of 7 BSI categories are shown because fungal BSIs and the
918 uninfected category have no corresponding bacterial stool abundances). **c,d** left: neighbor-joining
919 tree constructed from all NCBI RefSeq assemblies of *Staphylococcus aureus* genomes in
920 addition to isolates that were isolated from subjects highlighted in **a**. right: counts of perfect read
921 matches of shotgun metagenomic reads from stool samples, red: stool sample sequencing read
922 matches to WGS of isolates from the same patient, black: matches to other genomes.

923 **Supplementary Table 1: Clinical characteristics of patients with confirmed COVID-19 at**
924 **NYU Langone Health and Yale New Haven Hospital**

925

	NYU, N = 60	YALE, N = 36	926
Age (years)	51 ± 17.5	62.52 ± 19.72	
Sex (F M)	42% 58%	39% 61%	
Hospital course and Outcomes			
ICU Admission	53%	65%	
Pneumonia	42%	77%	
Diarrhea	13%	32%	
Intubation	36%	41%	
Sepsis	23%	18%	
Encephalopathy	12%	3%	
Death	5%	21%	
Length of stay (median, IQR)	37 (10-86)	27 (11-35.25)	
Risk Factors			
Cancer within 1 year	7%	4%	
Chronic Heart Disease	18%	36%	
Hypertension	38%	64%	
Chronic Lung Disease	7%	20%	
Immunosuppression	17%	4%	

927 **Supplementary Table 2: Clinical characteristics of COVID-19 patients at NYU Langone**
928 **Health and Yale New Haven Hospital with and without positive blood culture results (BSI).**

929

	BSI, N = 26	non-BSI N = 53
Hospital course and Outcomes		
ICU Admission	69%	64%
Pneumonia	73%	53%
Diarrhea	31%	64%
Intubation	58%	36%
Sepsis	35%	21%
Encephalopathy	19%	6%
Death	15%	9%
Length of stay (median, IQR)	59 (23-91.5)	22 (6-51)

930

931

932

933 **Supplementary Table 3: Shotgun metagenomic reads mapped to species identified in clinical blood cultures.** Dark grey shading:
 934 no sequencing reads from stool samples matched the species identified in clinical blood samples, light grey shading: species of the
 935 same genus but not the same species had non-zero read counts in stool samples. The relative abundance of identified species were
 936 contrasted with their mean abundances (log₁₀ ratio).
 937

Organism identified in blood	species identified in stool sample	Log ratio
<i>Bacteroides thetaiotaomicron</i>	Bacteroides_thetaiotaomicron_14-106904-2	2.92
<i>Enterococcus faecalis</i> Group D	Enterococcus_faecalis_LD33	1.8
<i>Escherichia coli</i>	Escherichia_coli_K-12_substr._W3110	2.2
<i>Escherichia coli</i>	Escherichia_coli_IAI39	1.6
<i>Escherichia coli</i>	Escherichia_coli_536	2.8
<i>Klebsiella pneumoniae</i>	Klebsiella_pneumoniae_KPNIH27	-1.7
<i>Lactobacillus species</i>	Lactobacillus_curvatus_WiKim38	3.9
<i>Pseudomonas aeruginosa</i>	Pseudomonas_aeruginosa_SJTD-1	3.3
<i>Serratia marcescens</i>	Serratia_marcescens_CAV1492	-0.2
<i>Staphylococcus aureus</i>	Staphylococcus_aureus_RF122	1.9
<i>Proteus mirabilis</i>	Proteus_mirabilis;t_Proteus_mirabilis_BB2000	0.56
<i>Acinetobacter lwoffii</i>	Acinetobacter_calcoaceticus_EGD_AQ_BF14	-0.6
<i>Staphylococcus</i>	Staphylococcus_sp._HMSC063G01_HMSC063G01	0.9
<i>Staphylococcus</i>	Staphylococcus_epidermidis_W23144	3.3
<i>Staphylococcus aureus</i>	not found	
<i>Staphylococcus hominis</i>	not found	
<i>Staphylococcus capitis</i>	not found	
<i>Staphylococcus epidermidis, hominis</i>	Staphylococcus_pseudintermedius_063228	2.2
<i>Staphylococcus epidermidis, hominis ssp hominis</i>	not found	
<i>Staphylococcus epidermidis</i>	Staphylococcus_aureus_JKD6008	2.7
<i>Staphylococcus epidermidis</i>	Staphylococcus_epidermidis_DAR1907	1.1
<i>Staphylococcus capitis</i>	Staphylococcus_sp._HMSC067F07_HMSC067F07	3.7
<i>Staphylococcus epidermidis, hominis ssp hominis</i>	Staphylococcus_hominis_793_SHAE	0.8
<i>Staphylococcus epidermidis</i>	Staphylococcus_sp._HMSC070D05_HMSC070D05	3.8
<i>Staphylococcus hominis, epidermidis</i>	Staphylococcus_hominis_MMP2	1.0
<i>Staphylococcus hominis, epidermidis</i>	Staphylococcus_epidermidis_ATCC12228_GCF7645.1	0.2

938

939 **Supplementary Table 4:** SRA accession numbers for the bioproject PRJNA745367

940 corresponding to the mouse sequencing data.

941 (Excel sheet)

942

943 **Supplementary Table 5:** SRA accession numbers for the bioproject PRJNA746322

944 corresponding to the human stool samples sequencing data.

945 (Excel sheet)

946